Dendrochronologia 55 (2019) 80–92

Contents lists available at ScienceDirect

Dendrochronologia

journal homepage: www.elsevier.com/locate/dendro

A 2917-year tree-ring-based reconstruction of precipitation for the Buerhanbuda Mts., Southeastern Qaidam Basin, China

Hongli Wang[a,b], Xuemei Shao[a,b,*], Mingqi Li[a,b]

[a] Key Laboratory of Land Surface Pattern and Simulation, Institute of Geographic Sciences and Natural Resources Research, Chinese Academy of Sciences, Beijing, China
[b] University of Chinese Academy of Sciences, Beijing, China

ARTICLE INFO

Keywords:
Tree-ring
Qaidam Basin
Millennium
Chronology
Annual precipitation
Climate change

ABSTRACT

In this study, we developed the tree-ring width chronology for the period of 1404 BCE to 2015 CE using Qilian juniper (*Sabina przewalskii* Kom.) trees collected from the Buerhanbuda Mts. in the southeastern Qaidam Basin (QB) near Nuomuhong Village, Qinghai Province. This is the first and longest chronology to date in this region. Based on the relationships between the tree-ring width chronology and climate data, the annual precipitation from previous July to current June (July-June) was reconstructed for the past 2917 years from 902 BCE to 2015 CE. This reconstruction accounted for 47.9% of the total variance in the actual July-June precipitation in the calibration period (1957–2015). The full reconstruction captured distinct wet and dry variability, and contained evidence of some low-frequency climate signals. We identified 13 wet and 12 dry periods, of which 1443–1503 CE and 1789–1836 CE were the two longest dry periods. General agreements in the low-frequency variations between the July-June precipitation and other moisture-sensitive records for the northeastern Tibetan Plateau (TP) suggested that the reconstruction in this study represented a regional signal. Spatial correlations with gridded precipitation data also indicated that the reconstructed July-June precipitation could adequately represent climate fluctuations over a large area of the northeastern TP. The new tree-ring width chronology and precipitation reconstruction are important for understanding natural climate change in the southeastern QB.

1. Introduction

Reconstruction of past climate using a variety of proxies is important for improving our understanding of natural climate variability (Mann et al., 2009), and quantifying the influence of external forcings and intrinsic dynamics of the global climate system (Snyder, 2010). Tree rings have been widely used to construct multi-century and multi-millennium chronologies that reveal local (site) (Shao et al., 2005; Knight et al., 2010; Allen et al., 2017), regional (combination of several sites within a region) (Büntgen et al., 2005, 2011; Yang et al., 2014), and hemispheric/global climatic fluctuations (Briffa et al., 2001; Cook et al., 2013; Esper et al., 2018). The importance of high-resolution and long time scale climate reconstruction is highlighted in the Fifth Assessment Report of Working Group 1 of the IPCC (Masson-Delmotte et al., 2013) and the Past Global Changes (PAGES) (Eddy, 1992). In recent decades, an increasing number of millennium-long tree-ring chronologies and climate reconstructions have been established from mid- to high- latitudes worldwide (Pilcher et al., 1984; Hughes and Graumlich, 1996; Cook et al., 2000; Grudd et al., 2002; Friedrich et al., 2004; Lara et al., 2005; Nicolussi et al., 2009). These long proxy records with annual resolution provide an excellent opportunity and reliable basic data for understanding the processes and mechanisms of historical climatic changes at sub-hemispheric scales.

In the northern Xinjiang (Tianshan Mts. and Altay Mts.) (Chen et al., 2014, 2016a), the Tibetan Plateau (TP) (Zhang et al., 2003; Yang et al., 2014; Chen et al., 2016b), the Hengduan Mts. (Fan et al., 2008; Yu et al., 2018), the Loess Plateau (Liu et al., 2004; Fang et al., 2012), Northeast China (Chen et al., 2012), and some regions in Southern China (Zhao et al., 2014; Xu et al., 2016), considerable improvements based on tree rings at century to millennium time scales have been achieved in the past two decades, especially in the arid regions of northwest China. Most of the millennium-long studies have been conducted in the TP and its surrounding areas, which provide valuable data for understanding the historical climatic changes and their driving mechanisms in the TP over the past millennia. These studies are mainly located in Qilian Mts. (Kang et al., 2002, 2003; Liu et al., 2005, 2007; Zhang et al., 2011b; Sun and Liu, 2012; Zhang et al., 2014), eastern Qaidam Basin (QB) (Kang et al., 2000; Zhang et al., 2003; Sheppard et al., 2004; Shao et al., 2005; Liu et al., 2006; Shao et al., 2006; Zhang and Qiu, 2007; Yin et al., 2008; Zhu et al., 2008; Liu et al., 2009; Shao

* Corresponding author.
E-mail address: shaoxm@igsnrr.ac.cn (X. Shao).

https://doi.org/10.1016/j.dendro.2019.04.002
Received 12 March 2019; Received in revised form 12 April 2019; Accepted 13 April 2019
Available online 17 April 2019
1125-7865/ © 2019 Elsevier GmbH. All rights reserved.

et al., 2009; Shi et al., 2009; Wang et al., 2013; Yang et al., 2014; Yin et al., 2016), Animaqing Mts. (Gou et al., 2010; Chen et al., 2016b), and southeastern TP (He et al., 2013; Wang et al., 2014, 2015; Nie et al., 2017). Most of the studies mentioned above focused on local/regional dry and wet changes (such as precipitation, soil moisture, stream flow, and SPEI index) (Kang et al., 2002; Yang et al., 2014; Yin et al., 2016; Nie et al., 2017). However, the number of 2000-year-long local-to-regional scale proxy series is very limited. There are only six series available, which are all developed based on Qilian juniper tree-ring width, and they are concentrated in the eastern QB (Zhang et al., 2003; Sheppard et al., 2004; Liu et al., 2009; Shao et al., 2010; Yang et al., 2014), except for the 2000-year temperature reconstruction in the Animaqing Mts. (Chen et al., 2016b). By far, the longest tree-ring width chronology, which spans 4500 years and represents annual precipitation changes since 1500 BCE, was constructed using subfossil, archaeological, and living Qilian juniper trees from the northeastern TP (Yang et al., 2014).

Qilian juniper is a species that has been recognized as one of the longest-lived conifers worldwide. Remnant or subfossil wood of this species could be preserved without decay in remote and extremely arid mountains where forests have been least affected by human activities. Therefore, living Qilian juniper trees, dead trees, and archeological wood samples obtained from the ancient tombs can be gradually spliced to develop records that are thousands of years long by tree-ring crossdating to monitor environmental changes at a variety of time scales. Encouraged by the previous work (Shao et al., 2009), we fortunately discovered a few new sites for sampling living trees, dead trees and snags on the eastern Buerhanbuda Mts., which were the westernmost spots in the southeastern part of the QB. According to the basic principle of limiting factors and the concept of ecological amplitude, trees growing near semiarid forest border sites are highly sensitive to climatic variations and have a higher research value than trees growing in areas with better moisture conditions (Fritts, 1976). Therefore, new tree-ring chronology in this extremely arid region is of significance to further our understanding about climatic changes at longer time scales and larger spatial scales.

The goal of this study was to present a long and reliable tree-ring width chronology based on Qilian juniper trees collected from the Buerhanbuda Mts.. According to the tree growth-climate relationships, we reconstructed the annual precipitation from previous July to current June for the past 2917 years. This is the first study to undertake a millennium-long chronology and climate reconstruction in the extremely arid forest border region, and it will provide valuable information on precipitation variability over the past millennia for the southeastern QB. The reconstruction could be compared to other moisture-sensitive series to obtain information about large-scale climate variations.

2. Materials and methods

2.1. Study area and tree-ring data

The study area was situated in the northeastern part of the TP in China (Fig. 1a). More specifically, it was located in the Buerhanbuda Mts. of the southeastern QB, approximately 60 km south of Nuomuhong Village and 150 km west of Dulan County, Qinghai Province (Fig. 1b). The climate in the basin belongs to a typical plateau-continental arid climate zone with distinct seasonality, and is dry throughout the year (Zheng, 1996). Based on the meteorological station in Nuomuhong (36.43 °N, 96.42 °E; 2790 m in elevation), which was the nearest station to the tree-ring sampling sites, the annual mean temperature was 5.02 °C with a mean January temperature of −9.60 °C and mean July temperature of 17.76 °C during the period of 1957–2016 (the climate data were collected from the National Meteorological Information Center of China). The annual precipitation was only 46.00 mm at Nuomuhong, while monthly total precipitation varied from 12.03 mm in June to 0.27 mm in November. For the Dulan (36.30 °N, 98.10 °E; 3191 m in elevation) meteorological station during the same period, the annual mean temperature was 3.22 °C with a mean January temperature of −9.85 °C and mean July temperature of 15.07 °C. The annual precipitation in Dulan was 203.06 mm with total precipitation of 45.58 mm in July and 3.00 mm in December, which was more than four times greater than that in Nuomuhong (Fig. 1c). It is clear that high temperature coincides with high precipitation during summer in the study area. Precipitation from May to September accounts approximately 90% of the annual precipitation, which is driven by both the mid-latitude Westerlies and Asian monsoons (Dai, 1990). Moreover, the annual mean temperature and annual precipitation increased significantly in the recent 50 years (Li et al., 2015).

The natural vegetation is sparse, and consists of various herbs and shrubs of desert species with rare forest stands (Fig. 2a and b) owing to the extremely arid climate conditions (Du and Sun, 1990). Qilian juniper is the only dominant drought-enduring tree species growing on the sunny and semi-sunny hillslopes at elevations of about 3500–4100 m in the Buerhanbuda Mts., where receive more precipitation because of the orographic effect (Du and Sun, 1990). Table 1 presents general information on the eight sampling sites used in this study. NMH (living trees) and NMHS (dead trees) were sampled in June 2003 and June 2005, respectively. Most of the data were used in constructing the 3585-year chronology in the eastern and northeastern QB (Shao et al., 2009). The oldest dead tree dated from NMHS was 752 years, covering 650 BCE to 202 CE, indicating the great potential of prolonging the multi-millennium chronology in the study area. Since 2012, repeated field work and sample collection has been undertaken to improve the replication of the existing samples and (potentially) to extend the record back in time. The cores were extracted using either 4.35 mm or 5.15 mm diameter increment borers in June 2012, August 2014, August 2015, and August 2016. Therefore, six additional sites were collected in hard-to-reach locations with different microenvironments (Fig. 1c). NMH3 was adjacent to NMH and NMHS with a distance of 0.5 km, but in different positions. NMH2, NMH5, NMH6, and NMH7 were nearby, with a distance of about 2 km among them, and were located southwest of NMH3. NMH8 was closest to the town, approximately 38 km from Nuomuhong. Among the eight sites, the largest distance between them (NMH8 and NMH2) was about 28 km. All the tree-ring samples used in this study were collected from sites of high elevation. We collected samples from almost every living tree, dead tree, and snag accessible on the hillside (Fig. 2c). This sampling strategy facilitated the replication of samples and crossdating of ring widths. Finally, a total of 602 increment cores from 274 Qilian juniper trees were collected to create the new chronology.

In the laboratory, all the increment cores were preliminarily processed following conventional dendrochronological techniques (Stokes and Smiley, 1968). The exact calendar year of each growth ring of living trees was assigned based on visual dating, and the ring width was measured at a resolution of 0.01 mm. For Qilian juniper trees growing in this extremely arid region, difficulties in crossdating arose from missing rings and from rings with indistinct boundaries, which were associated with the extremely slow growth rates of this species. The 3585-year (1580 BCE–2005 CE) ring-width chronology (Shao et al., 2009) was used as a reference during the process of crossdating for dead trees or snags in this study. When dating dead trees or snags, a section of ring widths with distinct boundaries was measured first, and then the COFECHA program (Holmes, 1983) was performed using undated series to give the hint of dating. Sections with indistinct ring boundaries were excluded; therefore, a core could be split into two or three segments. Through the splicing of living trees and dead trees, older trees could be crossdated progressively; thus, the record of precisely dated tree rings could be extended back to earlier periods.

After excluding some samples with abnormal ring features, such as excessive missing rings, broken pieces, or indistinct boundaries, crossdating and tree-ring width measurements were successfully completed

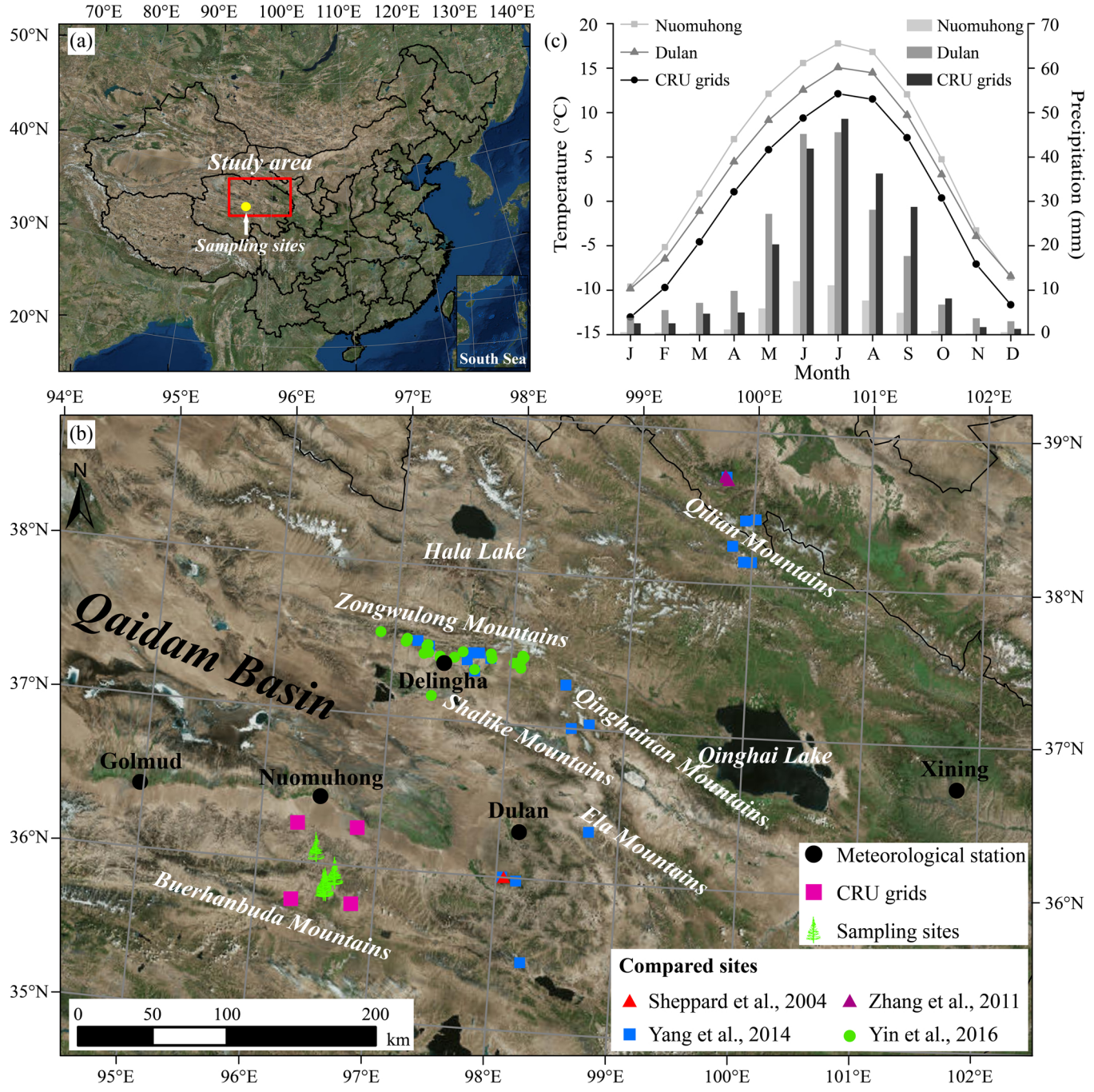

Fig. 1. (a) Location map of the study area. (b) Geographical positions of the sampling sites, meteorological stations, Climatic Research Unit (CRU) grid points, and sampling sites from other studies for comparison. (c) Climograph of the monthly mean temperature (dots connected by lines) and monthly total precipitation (columns) values of the Nuomuhong and Dulan meteorological stations and the average of four CRU grid points during the period of 1957–2016.

for a total of 458 cores from 222 trees. The cross-dated tree-ring series were quality checked for missing rings and dating errors with COFECHA program (Holmes, 1983). Some cores from dead trees with a deep color and complacent rings were excluded, because they could not be assigned an exact calendar year according to the current chronology. These samples may have been even older than the current chronology. From another perspective, this offered the possibility of extending the current chronology further back in time if old dead trees could be found in some spots in the study area. Table 1 also lists the tree-ring dating statistics. Except for NMH, which was the site based on living trees, the other seven sites all extended back to BCE.

2.2. Chronology development

To ensure the quality of the chronology, individual tree-ring width series having a low correlation coefficient value of 0.5 with the master series, were removed from the final chronology. Because the eight sampling sites were located in close geographic proximity, all of the crossdated individual series were merged to develop a single chronology. Ultimately, a total number of 455 cores from 222 trees were retained to develop the chronology in the present study.

From the data of ring width measurements, we noticed that more than 90% of the rings in this study were less than 0.5 mm in width. Following the suggestion by Cook and Peters (1997), a data-adaptive power transformation was first applied to the raw tree-ring data, and

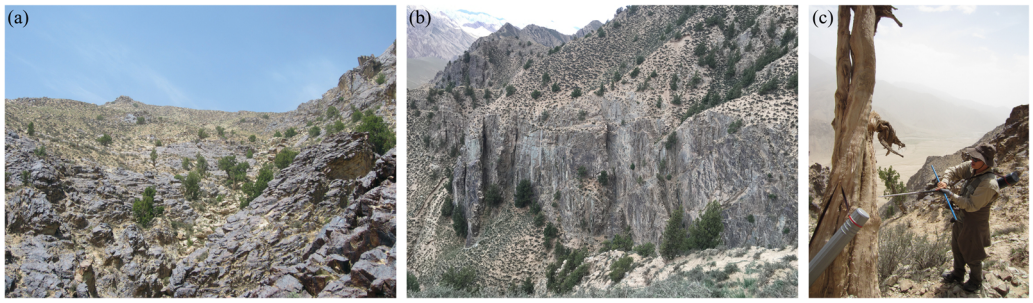

Fig. 2. Photographs of drought-stressed Qilian juniper trees. Sites overlooking (a) NMH6 (photo time: 08.12.2015) and (b) NMH7 (photo time: 07.30.2016). (c) View of an old-aged juniper tree at NMH6.

Table 1
Information of the eight sampling sites and their tree-ring dating characteristics.

Site code	NMH	NMHS	NMH2	NMH3	NMH5	NMH6	NMH7	NMH8
Lon. (E)	96.59°	96.59°	96.52°	96.58°	96.51°	96.51°	96.50°	96.41°
Lat. (N)	35.94°	35.94°	35.86°	35.94°	35.87°	35.86°	35.86°	36.09°
Alt (m)	3690	3686	3804	3840	3966	4098	4015	3600
Aspect	NE	SE	SE	SW	SE	SW	SW	SE
Slope	30°	30°	33°	36°	25°	35°	30°	30°
Sampling time	2003.6	2005.6	2014.8	2012.6	2014.8	2015.8	2016.7	2016.8
Samples collected	26/61	24/55	21/42	58/118	32/71	18/46	60/133	35/76
Samples dated	25/57	22/48	16/30	52/99	28/58	17/43	49/96	13/27
Time span	713 CE – 2002 CE	1289 BCE – 1828 CE	841 BCE – 2013 CE	1404 BCE – 2011 CE	931 BCE – 2014 CE	1041 BCE – 2014 CE	1101 BCE – 2015 CE	701 BCE – 2015 CE
ML (y)	267.2	254.3	198.9	264.9	200.7	254.0	296.4	234.7
PMR (%)	1.25	1.56	1.29	0.92	1.17	1.20	1.43	1.21
MS	0.41	0.43	0.44	0.39	0.41	0.43	0.47	0.41
MC	0.68	0.73	0.72	0.70	0.73	0.74	0.79	0.72
Site No. in Fig. 8	51	26	52	53	54	55	56	57

ML: mean length; PMR: percentage of missing rings; MS: mean sensitivity; MC: mean correlation with the master chronology.

the tree-ring indices were calculated as residuals between the measured raw tree-ring width after power transformation and the corresponding fitted values of the growth trend. This could stabilize the variance in ring-width series and reduce the potential bias in tree-ring indices (Cook and Peters, 1997). We used a negative exponential function or linear regression with a negative slope to fit the biological growth trend inherent in the raw data series to preserve low-frequency climate signals. For the cores with piths (visible inner arcs) or those showing a clear ascending trend in the first 40–60 years of growth (Xu and Shao, 2007), the general negative exponential curve or Hugershoff growth curve was employed (Warren, 1980). The detrended series were finally averaged biweightly to generate the ring-width index chronology using the ARSTAN program (Cook, 1985).

In order to better retain the low-frequency variations, the standard chronology (NMH_{STD}) was utilized in further analyses. The running robust average correlation (Rbar) and expressed population signal (EPS) were used to evaluate the quality of the chronology. Both Rbar and EPS were computed for 50-year moving windows with 25 overlap. We used the EPS value of 0.85 as the threshold value to assess the adequacy of replication in the early portion of the chronology (Wigley et al., 1984). Other statistics, such as mean sensitivity (MS), standard deviation (SD), variance explained by the first principal component (PC1), and signal-to-noise ratio (SNR), were also calculated for the common period to assess the dendroclimatic potential of the chronology (Fritts, 1976).

2.3. Climate data and tree growth-climate relationship

In this study, climate data were obtained from the Climatic Research Unit (CRU) Time-Series (TS) Version 4.01 worldwide dataset available on a 0.5°×0.5° grid (Harris and Jones, 2017). Four climate variables were used, including monthly total precipitation, monthly mean temperature (*T*mean), monthly mean maximum temperature (*T*max), and monthly mean minimum temperature (*T*min). We selected four grid cells (35.75 °N–36.25 °N, 96.25 °E–96.75 °E; Fig. 1b) near the sampling sites and then averaged them to form the climate series for the study area. Although the monthly CRU dataset spanned the period of 1901–2016, we truncated the grid data from June 1956 to focus on the most reliable data period considering the fact that the two nearest meteorological stations, namely Nuomuhong and Dulan, were built in June 1956 and April 1954, respectively.

Then, the response of tree radial growth to climate was identified using a Pearson correlation analysis between the ring-width chronology and climate variables. Since the growth of a tree tends to lag behind the climate (Fritts, 1976), the climate variables included the months from previous July to current September for the correlation analysis. The first-order differences of the data were also calculated to conduct the correlation analysis to confirm whether a climate-growth relationship existed in the high-frequency domain.

2.4. Climate reconstruction

After identifying the climate variable and the seasonality that had the highest correlation coefficient with the ring-width chronology, we

used a scatter plot to identify whether the relationships between them were linear or nonlinear. Then, a regression model was used for calibration. The skill of the calibration model was verified using the leave-one-out (Michaelsen, 1987) and split-period (Fritts, 1976) validation methods. Various statistics used for calibration and verification, including the Pearson correlation coefficient (*r*), sign tests of both the first difference (ST1) data and raw data (ST), reduction of error (RE), coefficient of efficiency (CE), and product mean test (PMT), were calculated to evaluate the similarity between the actual data and estimated data (Fritts, 1976). Any RE and CE values above 0 demonstrated rigorous model skill. To examine the spatial representation of the reconstruction during the common period, spatial correlations were conducted between both the actual and reconstructed precipitation with the CRU TS 4.01 dataset for the period of 1957–2015 using the KNMI climate explorer (Trouet and Oldenborgh, 2013). We also compared our reconstruction with typical proxy-based independent reconstructions of moisture to validate the reconstruction.

3. Results

3.1. Statistics of the NMH_{STD} chronology

The resulting NMH_{STD} chronology spanned the period of 1404 BCE to 2015 CE (Fig. 3a). As shown by the chronology statistics in Table 2, the NMH_{STD} chronology had high MS and SD values, thereby indicating that tree growth in the local environment was sensitive to climatic changes, and that the chronology reflected high interannual variations. The value of AC1 was 0.35, thereby indicating that tree radial growth in one year had an impact on the growth in the next year. There were 2307 local missing rings out of a total 186,416 measurement rings in the crossdated data set (1.249%). Over the past 3419 years, the number of years that contained at least one missing ring for a given year was 447, which ranged between one in the 13th century BCE and thirty in the 15th century CE. The number of years with missing rings decreased before the 8th century owing to the reduction in sample depth (Fig. 3b). At the same time, we found that there were three distinct low valleys in the sample depth in the 12th century, 15th century, and 19th century, which were also observed in the Dulan chronology (Zhang et al., 2003; Sheppard et al., 2004). The tree rings in the above three centuries showed extremely suppressed growth, which was often associated with distorted ring patterns that were narrow or with decades of rings that were completely inseparable and indistinguishable. However, the year with the most missing rings was 786 CE, in which there were 28 samples with missing rings out of the total of 38 dated samples.

For the common period of 801–1000 CE (28 dated series from 21 trees) (Table 2), the percent variance explained by PC1 was 46.7% and the SNR was 21.68, thereby suggesting that there was a strong common signal among the samples. According to the threshold for EPS greater than 0.85, the well-replicated period of the NMH_{STD} chronology started from 902 BCE, when there were at least eight cores available. The Rbar value and EPS value ranged from 0.27 to 0.62 and from 0.88 to 0.99, respectively, over the period of 902 BCE–2015 CE (Fig. 3c).

3.2. Correlations between the tree-ring index and climate factors

According to the results of the correlation analysis, tree growth of Qilian junipers in the study area showed a closer relationship with precipitation than temperature (Fig. 4). Positive correlations between the tree-ring index and precipitation were found from July to September of the previous year and from May to June of the current year. The results of the correlation analysis based on the first-order difference were almost similar to those based on the original data (Fig. 4a). In

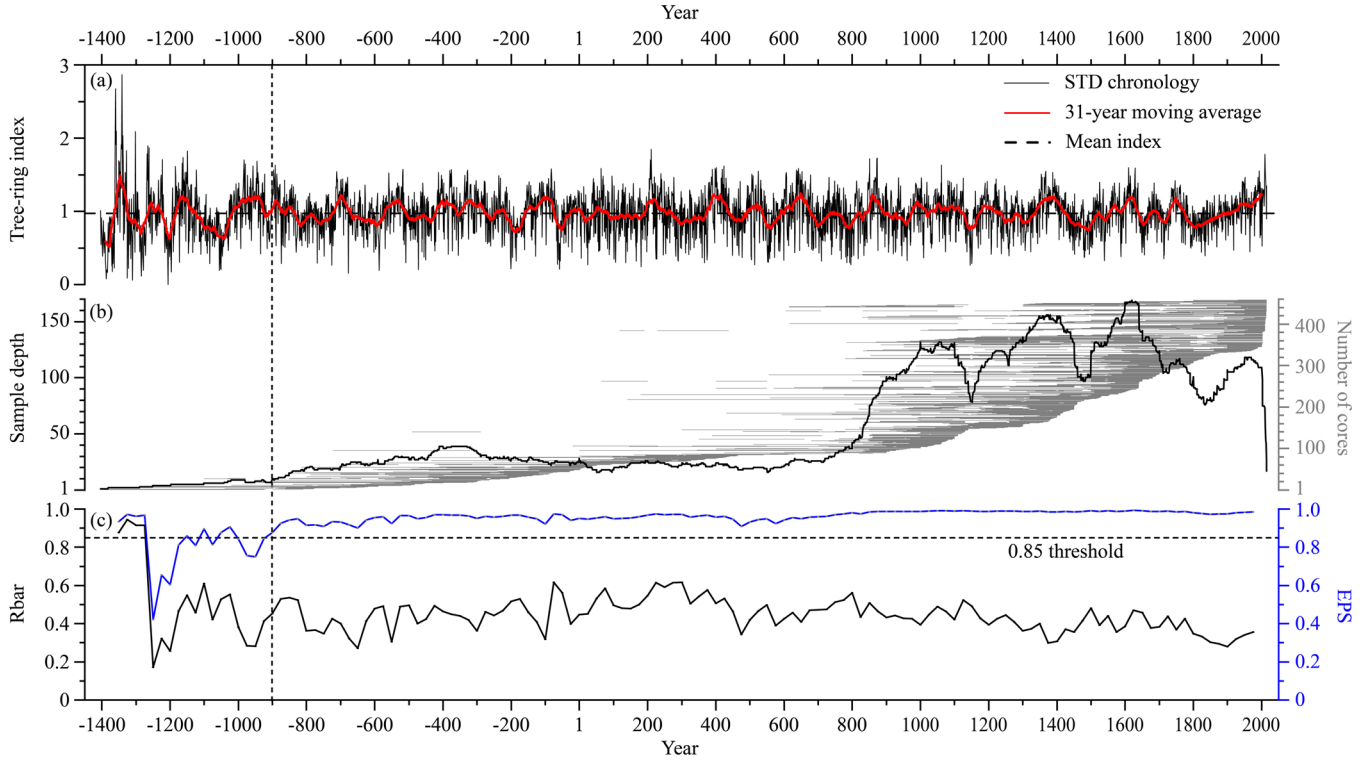

Fig. 3. Standardized tree-ring width chronology and its statistical parameters. (a) The NMH_{STD} chronology (black curve). The heavy red curve is the corresponding 31-year average smoothing series. The horizontal dotted line denotes the mean tree-ring index (0.97). (b) The change in sample depth over time (dark curve) and temporal distribution of sample cores (gray line); all the tree-ring series are ordered by the calendar age of their outermost ring. (c) The running robust average correlation (Rbar) (black curve) and expressed population signal (EPS) (blue curve). The horizontal dashed line denotes the 0.85 cutoff value. The vertical dashed line denotes the year 902 BCE, from when the EPS values exceeded the threshold of 0.85 (For interpretation of the references to colour in this figure legend, the reader is referred to the web version of this article).

Table 2
General characteristics of the NMH_{STD} and common interval analysis.

Entire chronology		Common interval analysis (801–1000 CE)	
Time span	1404 BCE–2015 CE	Correlation for all cores	0.44
Mean segment length	255.7	Correlation between trees	0.43
Percentage of missing rings	1.249%	Correlation within trees	0.88
Standard deviation	0.29	Signal-to-noise ratio	21.68
Mean sensitivity	0.30	Expressed population signal	0.96
1 st autocorrelation	0.35	Variance in 1 st eigenvector	46.70%

terms of temperature, the tree-ring index was negatively correlated with *T*mean from April to June of the current year, but the correlation was not significant (Fig. 4b). A significant positive correlation was found in the prior September for both the original data and the first-order difference data, and a significant negative correlation was found in the current June only for the first-order difference data. This negative correlation between tree radial growth and June temperature was even notable when we checked the results of *T*max (Fig. 4c). It was also found that the ring-width index was positively correlated with *T*min in all the months investigated, with significant positive correlations in the previous September to November and the current February to March (Fig. 4d).

Generally, the seasonal climate plays a more important role in tree growth than the climate of a single month. We combined different months of climate data to perform the correlation analysis with the tree-ring index. The results showed that the tree-ring chronology had the highest correlations with the annual precipitation summed from previous July to current June (July-June) ($r = 0.68$; $p < 0.01$), and the highest seasonal correlation with the sum of precipitation from the current May to June (May-June) ($r = 0.57$; $p < 0.01$). Further investigation of the relationship between the July-June precipitation and ring-width index indicated that they had a curve association (Fig. 5a), and the power of 2 transform of ring-width data produced the highest correlation between them.

3.3. Reconstruction and verification

Based on the above analysis, the annual precipitation summed from

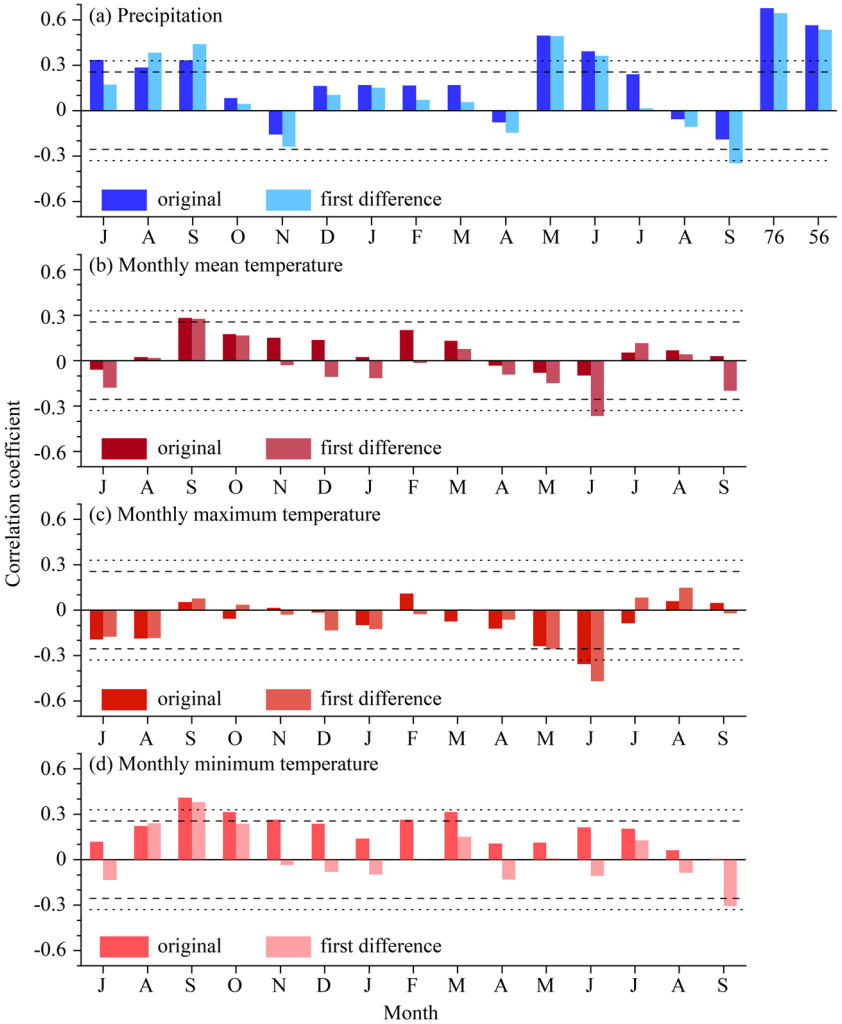
(a) Precipitation
(b) Monthly mean temperature
(c) Monthly maximum temperature
(d) Monthly minimum temperature
original
first difference
Correlation coefficient
Month
J A S O N D J F M A M J J A S 76 56

Fig. 4. The correlations between the original and first differenced NMH_{STD} chronology and climate variables from the previous July to the current September during the calibration period of 1957–2015. The horizontal dashed lines and dotted lines indicate the 95% and 99% confidence intervals, respectively. The notions "76" and "56" represent that the values were calculated from the previous July to the current June and from the current May to June, respectively.

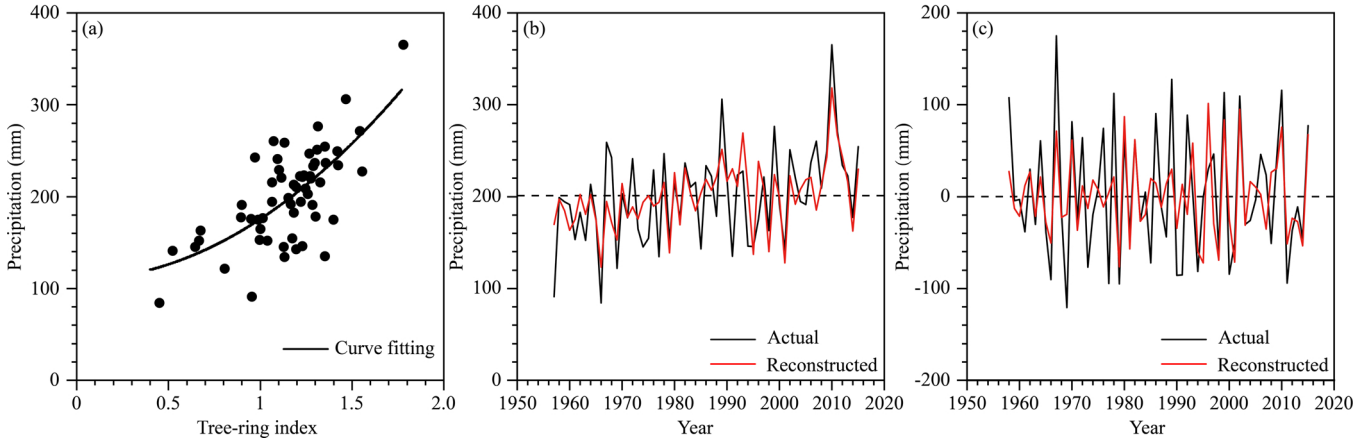

Fig. 5. (a) Scatter diagram and regression equation between precipitation and the tree-ring indices during the period of 1957–2015. (b) Comparison of the actual and reconstructed July-June precipitation for the common period (1957–2015). The horizontal dashed lines represent the mean values for the actual July-June precipitation from 1957 to 2015 (201.21 mm). (c) Comparison of the first differenced values for actual and reconstructed precipitation.

July of the previous year to June of the current year ($Pre_{P7\text{-}C6}$) was reconstructed from 902 BCE to 2015 CE. The transfer function was designed as follows:

$$Pre_{P7\text{-}C6} = 65.87 \times NMH_{STD}{}^2 + 109.96 \quad (1)$$

where NMH_{STD} is the tree-ring width chronology.

Table 3 shows the calibration and verification statistics. The quadratic model accounted for 47.9% of the actual July-June precipitation variance during the calibration period of 1957–2015 (Fig. 5a), even though the adjusted R^2 value decreased slightly to 47.0% and the F-test value was 52.50. The sign test (including the first difference sign test) and PMT values revealed that actual and reconstructed precipitation matched well for both the low and high-frequency variations. For the entire calibration period and two sub-periods, the results yielded positive RE and CE values, thereby indicating that the reconstruction was effective (Fritts, 1976). Fig. 5b shows the comparison of the actual July-June precipitation with the reconstructed precipitation in the calibration period. It can be seen that the reconstructed precipitation maintained the same trend as that of the actual data during the overlap period from 1957 to 2015, but there were differences between the amplitudes of the reconstructed and actual values. The quadratic equation fitted well not only to some low precipitation years, but also to some high precipitation years. We further compared the first differences in the reconstructed and actual precipitation; the correlation coefficient was 0.647 ($p < 0.01$; n = 58). Overall, these statistics strongly verified our regression model; thus, our reconstruction could represent the long-term precipitation variations in the Buerhanbuda Mts. over the past 2917 years.

To further reveal the regional response, we analyzed the spatial field correlation between the actual and reconstructed July-June precipitation and the CRU gridded precipitation over China during the common period of 1957–2015 (Fig. 6a and b). This spatial field correlation was also inspected using the first-order difference data of the reconstructed July-June precipitation and CRU gridded precipitation to view the associations in high frequency (Fig. 6c). The actual annual precipitation was significantly and positively correlated with the gridded precipitation over all of Qinghai Province (Fig. 6a). The spatial field correlations derived from the original and first-order difference data of the reconstructed precipitation and CRU gridded dataset generally displayed a similar pattern with that of the actual data, with somewhat lower correlation coefficients and a larger spatial coverage of statistical significance (Fig. 6b and c). Thus, these similarities confirmed that the chronology could be applied as a useful proxy for climate reconstruction, and that our precipitation reconstruction represented large-scale moisture variability in northwestern China.

3.4. Variability in annual precipitation

Based on the above transfer function, the annual precipitation (July-June) for the Buerhanbuda Mts. was reconstructed (Fig. 7). The full precipitation reconstruction (902 BCE–2015 CE) revealed strong interannual, multidecadal/centennial variations, thereby providing a valuable long series to evaluate the local climate variability. The mean precipitation was 177.59 mm, which was lower than that of the last 60 years, thereby indicating a wet condition in recent period. The five wettest years were 211 CE (334.17 mm), 2010 CE (318.18 mm), 873 CE (306.63 mm), 851 CE (304.82 mm), and 872 CE (303.23 mm), and the five driest years were 677 BCE (111.50 mm), 587 BCE (112.39 mm), 472 BCE (112.68 mm), 59 BCE (112.92 mm), and 201 BCE (112.98 mm). The wettest and driest decades were the 640 s (640–649 CE; average annual precipitation 221.74 mm, the same below) and 550 s (550–559 CE; 138.28 mm), respectively. Additionally, the wettest and driest centuries were the 7th century (190.90 mm) and 15th

Table 3
Calibration and verification statistics of the reconstruction model.

Calibration				Verification						
Period	R^2	$R_{adj}{}^2$	F	Period	r	ST	ST1	PMT	RE	CE
1957–2015	0.479**	0.470	52.50	1957–2015	0.66	43+/16-**	44+/14-**	2.62	0.44	–
1957–1986	0.355**	0.332	15.43	1987–2015	0.69	24+/5-**	20+/8-*	2.05	0.61	0.45
1986–2015	0.482**	0.464	26.06	1957–1985	0.58	24+/5-**	22+/6-**	2.54	0.55	0.28

R^2: explained variance; $R_{adj}{}^2$: explained variance after the degree of freedom is adjusted; F: statistical significance of the regression models; r: Pearson correlation coefficient of the original-reconstructed climate in the verification period; ST: sign test; ST1: the first difference sign test; PMT: the t value derived using the product mean test; RE: reduction of error; CE: coefficient of efficiency; **: $p < 0.01$; *: $p < 0.05$.

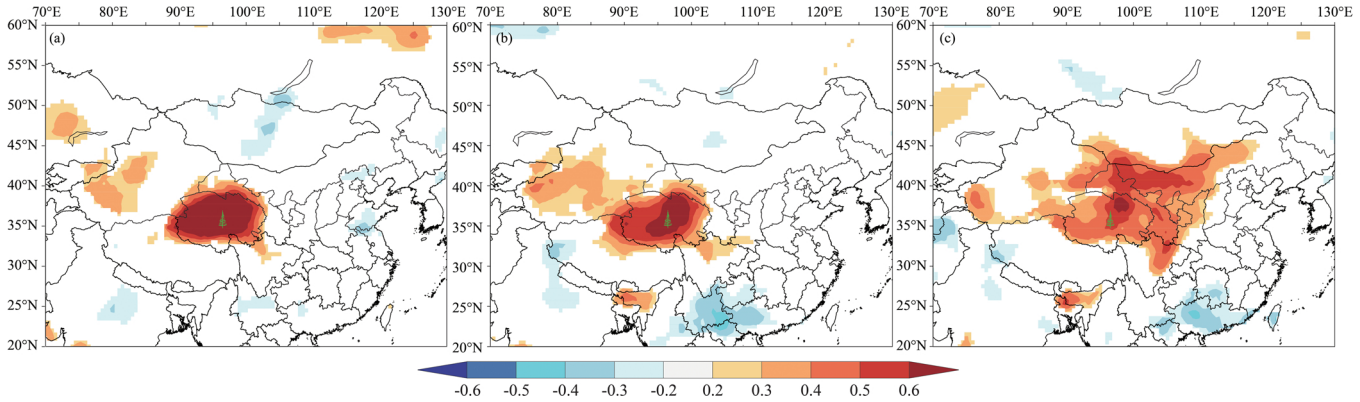

Fig. 6. Spatial correlations between the (a) actual and (b) reconstructed annual precipitation (July-June) and the gridded annual precipitation (Climatic Research Unit (CRU) Time-Series (TS) 4.01) for the period of 1957–2015. (c) The first differenced correlations between the reconstructed precipitation and the CRU gridded July-June precipitation for the period of 1959 – 2015. The green trees represent the location of the sampling sites. The colored areas indicate the areas with significant correlations ($p < 0.1$). The scale on the bottom shows the correlation coefficients represented by different colors (For interpretation of the references to colour in this figure legend, the reader is referred to the web version of this article).

century (162.99 mm), respectively, while the wettest and driest hundred years were 1916–2015 CE (195.88 mm) and 1774–1873 CE (159.17 mm), respectively.

A value of +1.5σ (σ = 33.75 mm) above the mean designated an extremely wet year ($Pre_{P7\text{-}C6} > 228.22$ mm), and an extremely dry year was identified as –1.5σ below the mean ($Pre_{P7\text{-}C6} < 126.96$ mm). Since 902 BCE, 225 years were identified as extreme wet years (average precipitation 246.86 mm), which accounted for 7.71% of the total, and 152 years were identified as extreme dry years (average precipitation 120.92 mm), which accounted for 5.21% of the total. The decadal variability was highlighted by applying a 31-year moving average to the July-June reconstruction (Fig. 7). There were distinct alternations of dry/wet periods, thereby showing that the climate conditions varied considerably over the past three millennia from 887 BCE to 2000 CE. The wet/dry periods were the years where smoothed series exceeded or dropped below the mean ± 0.5σ, and the remaining years were categorized as normal years. The results showed that there were 13 wet periods and 12 dry periods with a duration of more than 10 years (Table 4). The five prominent wet periods that lasted more than 30 years were 118–80 BCE (39 years), 198–227 CE (30 years), 385–428 CE (44 years), 627–666 CE (40 years), and 1351–1403 CE (53 years). There were three notable dry periods, which were 201 – 168 BCE (34 years), 1440–1503 CE (61 years), and 1789–1836 CE (48 years).

Table 4
Listing of the decadal-scale wet and dry periods.

No.	Wet period		Dry period	
	Time	Duration (mean precipitation (mm))	Time	Duration (mean precipitation (mm))
1	710–685 BCE	26 (204.83)	823–806 BCE	18 (152.81)
2	537–524 BCE	14 (200.77)	764–754 BCE	11 (150.93)
3	395–386 BCE	10 (186.88)	601–587 BCE	15 (155.11)
4	333–314 BCE	20 (204.45)	201–168 BCE	34 (112.98)
5	118–80 BCE	39 (207.46)	61–44 BCE	18 (150.91)
6	198–227 CE	30 (201.66)	548–569 CE	22 (151.45)
7	385–428 CE	44 (208.11)	694–708 CE	15 (161.58)
8	627–666 CE	40 (206.04)	781–797 CE	17 (150.95)
9	852–880 CE	29 (202.56)	1136–1163 CE	27 (153.91)
10	1351–1403 CE	53 (205.61)	1443–1503 CE	61 (153.45)
11	1603–1628 CE	26 (207.20)	1650–1663 CE	14 (153.58)
12	1743–1754 CE	12 (202.65)	1789–1836 CE	48 (153.51)
13	1976–2000 CE	25 (205.64)		

The mean precipitation was calculated from the unsmoothed annual precipitation values. The wet/dry periods were identified using the smoothed series.

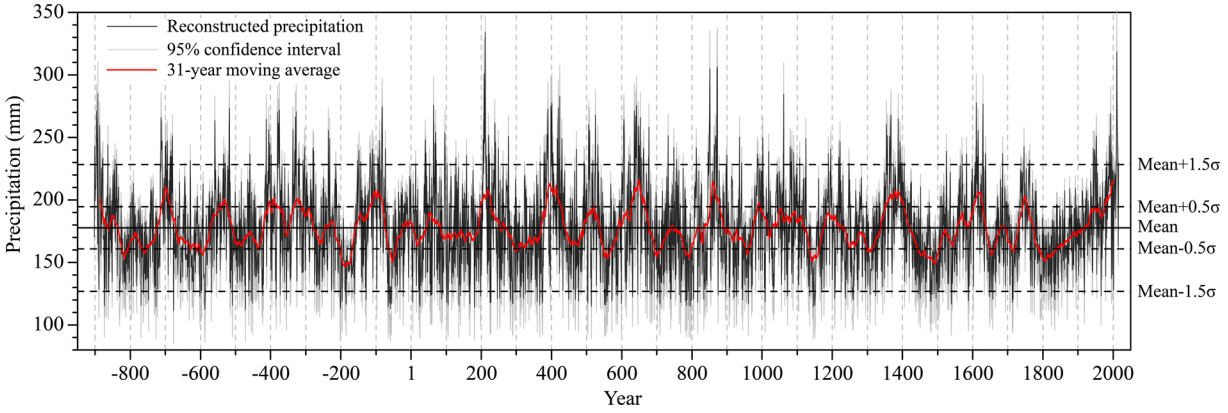

Fig. 7. Reconstructed annual precipitation (July-June) since 902 BCE (thin line) for Nuomuhong in the southeastern Qaidam Basin and its 31-year moving average (red curve). The thin gray line represents the 95% confidence interval. The solid horizontal line represents the long-term mean for the period of 902 BCE–2015 CE; the dashed horizontal black lines represent the mean ± 0.5σ and mean ± 1.5σ, respectively (For interpretation of the references to colour in this figure legend, the reader is referred to the web version of this article).

4. Discussion

4.1. The statistical characteristics of tree-ring widths in the extremely arid forest border sites

It has been shown that the chronology developed in the current study was based on samples from trees or snags that were scatter-distributed, thereby indicating a more arid environment for tree growth compared with the other long chronologies, such as the Dulan chronology (Zhang et al., 2003) and Delingha chronology (Shao et al., 2010) established to the east of the current study area. According to the study by Fritts (1976, pp 301), samples collected from extremely arid forest border sites may have a low correlation of ring widths among trees, high mean sensitivity, and more missing rings. In this study, the Qilian juniper trees are growing in arid forest border region and their radial growth rate is very slow. In some periods, the ring widths were too narrow to distinguish the rings with their adjacent ones, and there were even many partial or absent rings, creating extreme difficulty in crossdating. These problematic segments were excluded from further analysis in this study.

To evaluate the crossdating quality of our samples, the tree-ring statistics, including MS, mean correlation, and percentage of missing rings, for the eight sites under study were compared with those of 27 sampling sites of living or dead trees in the eastern and northeastern parts of the QB (Table 1 from Shao et al., 2009). It can be seen from Fig. 8, which shows the ring width index data of these sites, that in the current study, the correlations between ring widths among trees were not the lowest and the mean sensitivity and percentage of missing rings were not the highest, but instead were at a medium level, thereby indicating the acceptable quality of the data. At the same time, we found that the mean segment length of the series was only 255.7 years, which was the shortest among the chronologies in the eastern QB owing to the side effect of discarding the problematic segments. Nevertheless, this length was long enough to investigate interannual to multi-decadal variations, as well as centennial-scale variations (Cook et al., 1995). This study sets an example for developing long chronologies in extremely arid forest border sites.

4.2. Tree growth-climate relationships and the non-linear reconstruction model

The correlation analysis revealed a robust relationship between tree growth and precipitation, which confirmed that moisture availability was a consistently dominant climatic factor accounting for the interannual variation in tree-ring widths in the southeastern QB (Fig. 4). Moreover, the biophysical environment and the high incidence of missing rings in the study area also implied that tree growth was limited by moisture availability. Shao et al. (2005) indicated that the cambium of Qilian juniper started to be active at the end of May, and the earlywood should be largely formed by the end of June or early July. Adequate precipitation in growing season not only provides the main source of water for tree growth which may compensate the soil water deficit due to evapotranspiration, but also increases the total photosynthesis efficiency and stimulates the growth and division of tree cell to form a wider tree ring (Fritts, 1976). Studies on tree-ring widths and climatic conditions for conifers in arid and semi-arid sites have demonstrated that tree growth is not only influenced by the climate during the growing season, but also affected by the climate in the autumn, winter, and spring prior to the growing season (Fritts, 1976). The tree-ring index of this study was positively correlated with precipitation in previous late autumn and winter which emphasized the importance of soil moisture on tree growth, since more precipitation (most in form of snow) was probably stored in the underground and could serve as a water supply that would be conducive to facilitate tree growth in the coming growing season. Although precipitation had positive effects on the growth of Qilian juniper trees during the pre-growing season, the effect of precipitation during the active growing season was stronger. A similar positive response to precipitation was also reported for other arid and semi-arid sites in the northeastern TP (Zhang et al., 2003; Sheppard et al., 2004; Liu et al., 2006; Huang and Zhang, 2007; Yang et al., 2014), Qilian Mts. (Zhang et al., 2011b; Gou et al., 2015a, 2015b), and other mountainous regions in north-central China (Fang et al., 2012; Liu et al., 2013), Central Asia (Chen et al., 2014), and the Nepal Himalayas (Cook et al., 2003; Gairea et al., 2017).

In addition, the negative correlations between tree growth and

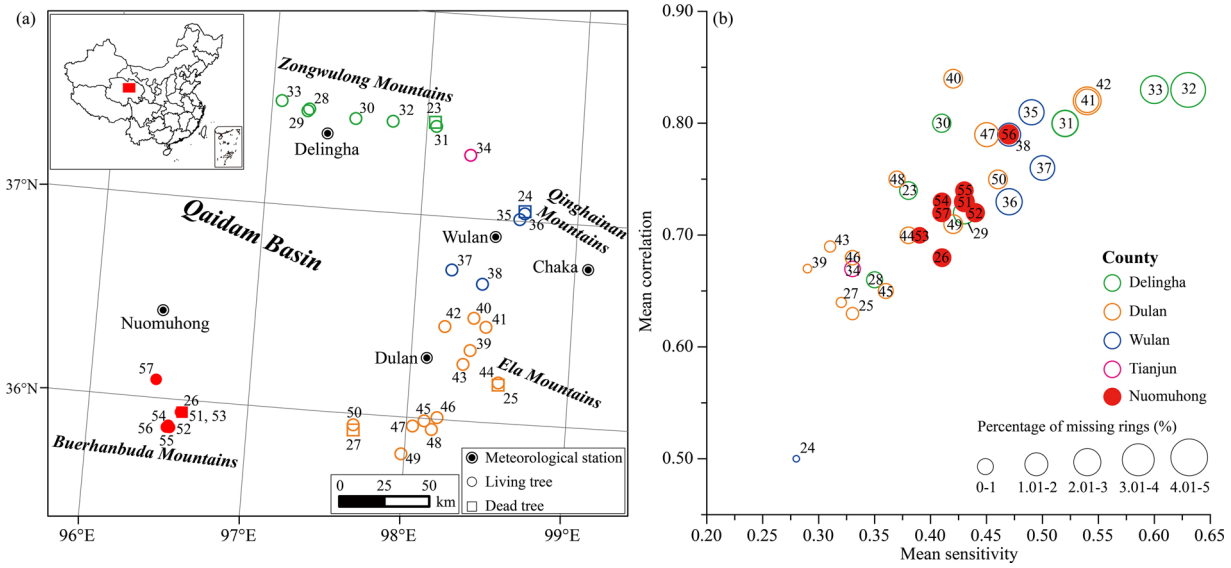

Fig. 8. (a) Location map of the 35 tree-ring sampling sites in the eastern part of the Qaidam Basin; sites 23–51 are identified in Table 1 from Shao et al. (2009) (samples collected from the tomb are excluded in this study). NMHS and NMH follow the site numbers in Shao et al. (2009), which are 26 and 51, respectively. Sites 52–57 represent the sampling sites NMH2, NMH3, NMH5, NMH6, NMH7, and NMH8, respectively. (b) The tree-ring characteristics of these 35 sampling sites including mean sensitivity (*x*-axis), mean correlation (*y*-axis), percentage of missing rings (area of the circle), and their geographical classification. The eight sampling sites of this study should be classified as Dulan County, but we listed the Nuomuhong sampling sites separately for visual analysis.

temperature (*T*mean and *T*max) during the growing season indicate that temperature has a limiting effect on the tree growth which is mainly due to strong evaporation caused by the increasing temperature. Previous studies of the same genus or at the same high altitude study regions also supported the possibility of climate-growth relationships between previous autumn and winter temperature (*T*mean and *T*min) and earlywood parameters (Gou et al., 2007; Zhu et al., 2008; Chen et al., 2016b; Li and Li, 2017). On the one hand, warm winter could protect roots from cold damage close to extreme for Qilian juniper trees. On the other hand, low temperatures may lead to thicker snow cover, which melts far more slowly in spring, and hence, delayed initiation of growth in the following spring which reduced earlywood widths (Fritts, 1976).

In general, a linear relationship between the year-to-year variation in the indices of tree-ring width and climate variables has been assumed and confirmed in a large number of tree-ring based climate reconstructions (Liu et al., 2009; Touchan et al., 2011; Arsalani et al., 2018). However, in this study, we found that a positive and non-linear association between the tree-ring index and actual precipitation was apparent with the tree-ring index becoming increasingly (decreasingly) sensitive as precipitation decreased (increased) through a scatter plot (Fig. 5a). Under the extremely arid climate conditions, precipitation was the major climate factor limiting tree growth. When precipitation was insufficient, tree growth was severely restricted, resulting in a narrow ring or absent ring; on the contrary, the trees grew faster and produced wide rings when the precipitation was sufficient. However, even the wide ring width often inadequately represented the wettest years. The process of reconstructing climate elements using linear regressions is characterized by a serious limitation, that is, there are large deviations between the fitted and actual values at high values, which is defined as wet bias (Sun et al., 2017). Virtually stream flow reconstructions based on tree-ring records have exhibited this bias. Some stream flow reconstructions used a simple nonlinear quadratic transformation to reduce the bias (Cleaveland, 2000; Graham and Hughes, 2007). In our study, the linear regression calibrated 45.6% of the actual precipitation variance during the period of 1957–2015. Quadratic transformation of the tree-ring series with a linear term improved the calibration to 47.9%, thereby emphasizing the increase in precipitation characterized by wide annual rings. Using a linear approach can be more practical than using complex nonlinear models, and it inherits interpretability from commonly used linear regressions.

4.3. Comparisons with other reconstructions

It can be seen from Fig. 3 that the ring-width indices in most years in the calibration period (1957–2015) (48 years out of 59 years) was above the mean value for the entire period from 1404 BCE to 2015 CE for the NMH_{STD} chronology, and it is mentioned in Section 3.4 that the wettest year occurred in 677 BCE and the driest year occurred in 211 CE in the reconstruction period. All of these may suggest that the entire range of variability in annual precipitation that occurred in the past is not included in the variations in the present day (calibration period) in the study area. To assess whether the annual precipitation reconstruction was appropriate, we conducted comparisons between the July-June reconstruction in this study and several other moisture-sensitive records (Fig. 9). The tree-ring data used in this study were completely independent of the series involved in the comparison. The precipitation series reconstructed in this study was significantly correlated with the Dulan tree-ring width chronology ($r = 0.346$, $p < 0.01$; n = 1621, 373–1993 CE) (Sheppard et al., 2004) (Fig. 9b), the tree-ring-based January-June moisture balance in the northeastern QB ($r = 0.525$, $p < 0.01$; n = 2847, 843 BCE–2004 CE) (Yin et al., 2016) (Fig. 9c), the annual precipitation reconstruction in the northeastern TP ($r = 0.540$, $p < 0.01$; n = 2913, 902 BCE–2011 CE) (Yang et al., 2014) (Fig. 9d), and the annual precipitation in the central Qilian Mts. ($r = 0.301$, $p < 0.01$; n = 1232, 775–2006 CE) (Zhang et al., 2011b) (Fig. 9e) at an interannual scale.

For better visual comparison, a 31-year average smoothing was employed to highlight the common low-frequency climate signals. As shown in Fig. 9, our new reconstructed precipitation showed similar dry and wet changes at a decadal scale compared to other records, especially during the dry periods. The two extreme and long-lasting drought events (1443–1503 CE and 1789–1836 CE) were depicted by almost all the series selected for comparison, thereby indicating the widespread occurrence of the devastating events over the northeastern TP during the Little Ice Age (Lamb, 1982). However, the duration and intensity of the two drought events were slightly different. Many other paleoclimatic reconstructions reflecting moisture conditions from Xinjiang (Zhang et al., 2011a), the southeastern TP (Liu et al., 2012; Grießinger et al., 2016; Nie et al., 2017), northeastern TP (Sun and Liu, 2012; Yin et al., 2016), and central China (Zhang et al., 2008) also showed these megadroughts, thereby suggesting that similar climate forcings may exist for large-scale drought variability over a large geographic area. They can also be observed in central Europe (Büntgen et al., 2011), Mongolia (Hessl et al., 2018), and the western USA (Grissino-Mayer, 1996; Knight et al., 2010). It is worth noting that the 31-year moving average precipitation has increased gradually since approximately the beginning of the 19th century, and the precipitation has exceeded the millennium average since the early 20th century. This rapid growth increase could not be attributed to the age structure of the studied trees used in developing the chronology because a homogenous age distribution of trees is indicated in Fig. 3b, and we also used a detrending procedure (see Section 2.2 for details) that was suggested to be free of the 'end effect' problem (Cook and Peters, 1997). These intensified wet conditions over the past century have been confirmed by other reconstructions in the northeastern TP (Shao et al., 2005; Yin et al., 2008; Zhang et al., 2011b; Yang et al., 2014), southeastern TP (He et al., 2018), central China (Zhang et al., 2008), and Mongolia (Davi et al., 2009).

Nevertheless, not all reconstructions matched perfectly; there were some unconformities in these series which may have been caused by differences in the microhabitat of different sampling sites, different detrending methods, or reconstruction uncertainties. Despite some differences in duration or intensity, the above comparisons suggest that our reconstruction not only provides a record of the regional moisture variability, but also reflects the climate variations in the northeastern TP, which will be useful for understanding regional climate change and its possible forcing mechanism.

5. Conclusion

In this study, a 3419-year tree-ring width chronology was successfully developed for the Buerhanbuda Mts., thereby indicating that there is great potential and feasibility to develop millennium-long tree-ring series in the extremely arid forest border region. It is currently the longest and most replicated tree-ring width chronology for the southeastern QB. The correlation analysis showed that tree growth was most strongly related to precipitation. As a result, the annual precipitation from previous July to current June over the past 2917 years was reconstructed based on the new tree-ring width chronology which was considered reliable since 902 BCE. This preliminary reconstruction provides valuable new information about climate change in the study area. Spatial field correlations with the gridded precipitation dataset revealed that the reconstruction captured large-scale regional moisture variations for the northeastern TP and its vicinity. The variation in the reconstruction corresponded well with some moisture-related records in different regions, especially during the drought periods, thereby indicating the coherency of both spatial and temporal scales. Overall, the new chronology expanded the spatial coverage of millennium tree-ring chronologies in the northeastern TP, which is helpful for improving the tree-ring databank of China.

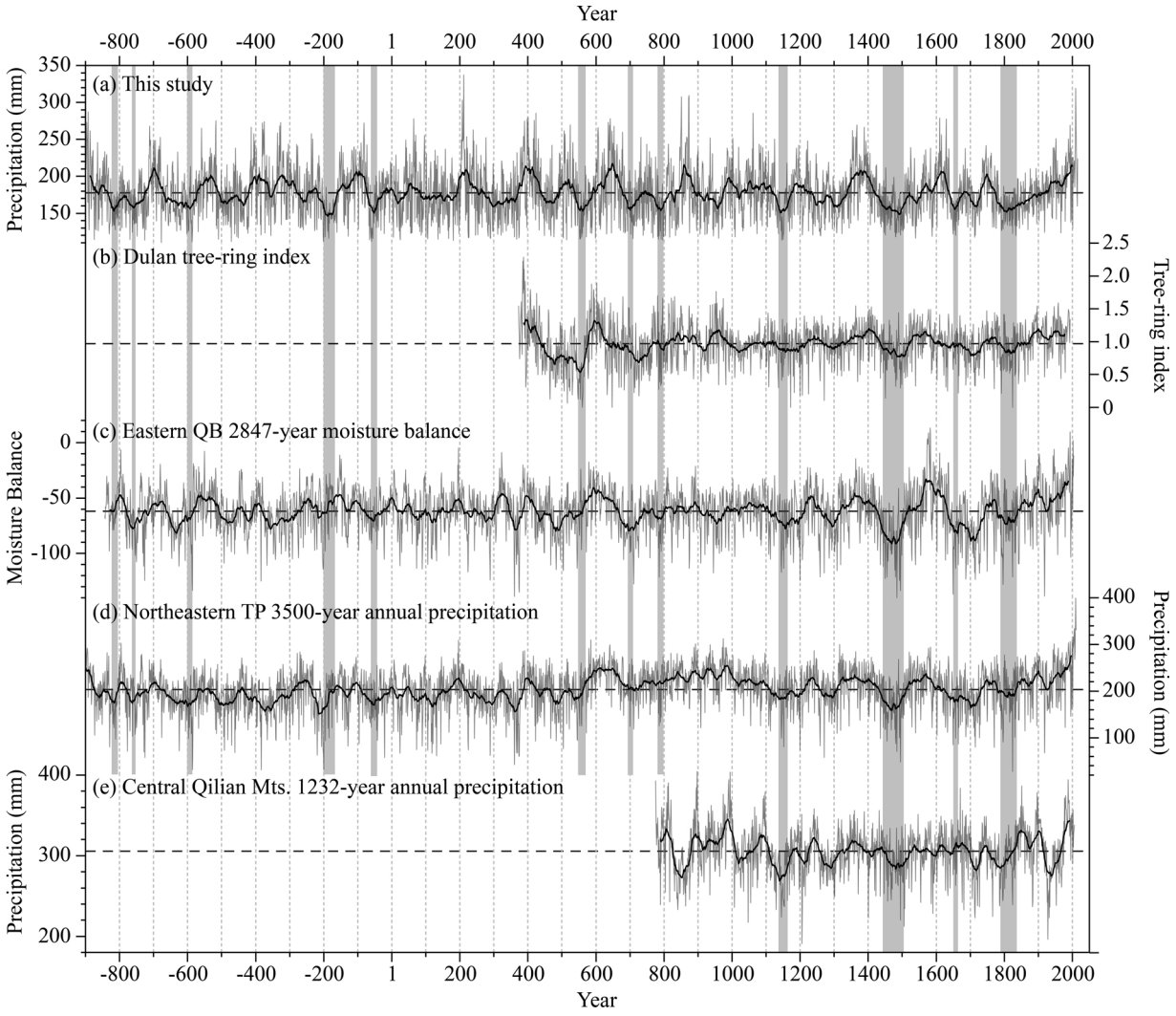
Year
-800 -600 -400 -200 1 200 400 600 800 1000 1200 1400 1600 1800 2000
(a) This study
Precipitation (mm)
350 300 250 200 150
(b) Dulan tree-ring index
Tree-ring index
2.5 2.0 1.5 1.0 0.5 0
(c) Eastern QB 2847-year moisture balance
Moisture Balance
0 -50 -100
(d) Northeastern TP 3500-year annual precipitation
Precipitation (mm)
400 300 200 100
(e) Central Qilian Mts. 1232-year annual precipitation
Precipitation (mm)
400 300 200
-800 -600 -400 -200 1 200 400 600 800 1000 1200 1400 1600 1800 2000
Year

Fig. 9. Comparisons among (a) the reconstructed $Pre_{P7\text{-}C6}$ in this study (902 BCE–2015 CE), (b) the Dulan tree-ring width index (Sheppard et al., 2004), (c) the 2847-year reconstructed moisture conditions in the eastern Qaidam Basin (QB) (Yin et al., 2016), (d) the 3500-year annual precipitation in the northeastern Tibetan Plateau (TP) (Yang et al., 2014), and (e) the 1232-year record of annual precipitation in the central Qilian Mts. (Zhang et al., 2011b). The dry periods are shaded in gray.

Conflict of interest

The authors declare that they have no conflict of interest.

Funding

This work was supported by the National Key R&D Program of China [grant number 2016YFA0600401]; the National Natural Science Foundation of China [grant numbers 41630529 and 41471170].

Acknowledgements

The authors wish to thank the Climatic Research Unit (CRU) for providing us with climate data. We would like to thank the members working in the Tree-ring and Paleoenvironment Research lab of Institute of Geographic Sciences and Natural Resources Research, Chinese Academy of Science for their help during crossdating and core measurement. We also thank the editors and two anonymous reviewers for their helpful comments that improved this work.

References

Allen, K.J., Fenwick, P., Palmer, J.G., Nichols, S.C., Cook, E.R., Buckley, B.M., Baker, P.J., 2017. A 1700-year *Athrotaxis selaginoides* tree-ring width chronology from south-eastern Australia. Dendrochronologia 45, 90–100. https://doi.org/10.1016/j.dendro.2017.07.004.

Arsalani, M., Pourtahamsi, K., Azizi, G., Bräuning, A., Mohammadi, H., 2018. Tree-ring based December-February precipitation reconstruction in the southern Zagros Mountains, Iran. Dendrochronologia 49, 45–56. https://doi.org/10.1016/j.dendro.2018.03.002.

Briffa, K.R., Osborn, T.J., Schweingruber, F.H., Harris, I.C., Jones, P.D., Shiyatov, S.G., Vaganov, E.A., 2001. Low-frequency temperature variations from a northern tree ring density network. J. Geophys. Res. Atmos. 106 (D3), 2929–2941. https://doi.org/10.1029/2000JD900617.

Büntgen, U., Esper, J., Frank, D.C., Nicolussi, K., Schmidhalter, M., 2005. A 1052-year tree-ring proxy for Alpine summer temperatures. Clim. Dynam. 25 (2-3), 141–153. https://doi.org/10.1007/s00382-005-0028-1.

Büntgen, U., Tegel, W., Nicolussi, K., Mccormick, M., Frank, D., Trouet, V., Kaplan, J.O., Herzig, F., Heussner, K.U., Wanner, H., 2011. 2500 years of european climate variability and human susceptibility. Science 331 (6017), 578–582. https://doi.org/10.1126/science.1197175.

Chen, Z.J., Zhang, X.L., Cui, M.X., He, X.Y., Ding, W.H., Peng, J.J., 2012. Tree-ring based precipitation reconstruction for the forest-steppe ecotone in northern Inner Mongolia, China and its linkages to the Pacific Ocean variability. Glob. Planet. Change 86-87, 45–56. https://doi.org/10.1016/j.gloplacha.2012.01.009.

Chen, F., Yuan, Y.J., Wei, W.S., Zhang, T.W., Shang, H.M., Zhang, R.B., 2014.

Precipitation reconstruction for the southern Altay Mountains (China) from tree rings of Siberian spruce, reveals recent wetting trend. Dendrochronologia 32 (3), 266–272. https://doi.org/10.1016/j.dendro.2014.06.003.
Chen, F., Shang, H.M., Yuan, Y.J., 2016a. Dry/wet variations in the eastern Tien Shan (China) since AD 1725 based on Schrenk spruce (*Picea schrenkiana* Fisch. et Mey) tree rings. Dendrochronologia 40, 110–116. https://doi.org/10.1016/j.dendro.2016.07.003.
Chen, F., Zhang, Y., Shao, X.M., Li, M.Q., Yin, Z.Y., 2016b. A 2000-year temperature reconstruction in the Animaqin Mountains of Tibet Plateau, China. Holocene 26 (12), 1904–1913. https://doi.org/10.1177/0959683616646187.
Cleaveland, M.K., 2000. A 963-year reconstruction of summer (JJA) stream flow in the White River, Arkansas, USA, from tree-rings. Holocene 10 (1), 33–41. https://doi.org/10.1191/095968300666157027.
Cook, E.R., 1985. A Time Series Analysis Approach to Tree Ring Standardization. Dissertation. University of Arizona.
Cook, E.R., Peters, K., 1997. Calculating unbiased tree-ring indices for the study of climatic and environmental change. Holocene 7 (3), 361–370. https://doi.org/10.1177/095968369700700314.
Cook, E.R., Briffa, K.R., Meko, D.M., Graybill, D.A., Funkhouser, G., 1995. The' segment length curse' in long tree-ring chronology development for palaeoclimatic studies. Holocene 5 (2), 229–237. https://doi.org/10.1177/095968369500500211.
Cook, E.R., Buckley, B.M., D'Arrigo, R.D., Peterson, M.J., 2000. Warm-season temperatures since 1600 BC reconstructed from Tasmanian tree rings and their relationship to large-scale sea surface temperature anomalies. Clim. Dynam. 16 (2-3), 79–91. https://doi.org/10.1007/s003820050006.
Cook, E.R., Krusic, P.J., Jones, P.D., 2003. Dendroclimatic signals in long tree-ring chronologies from the Himalayas of Nepal. Int. J. Climatol. 23 (7), 707–732. https://doi.org/10.1002/joc.911.
Cook, E.R., Krusic, P.J., Anchukaitis, K.J., Buckley, B.M., Nakatsuka, T., Sano, M., et al., 2013. Tree-ring reconstructed summer temperature anomalies for temperate East Asia since 800 CE. Clim. Dynam. 41 (11-12), 2957–2972. https://doi.org/10.1007/s00382-012-1611-x.
Dai, J.X., 1990. The Climate of the Tibetan Plateau. China Meteorological Press, Beijing.
Davi, N.K., Jacoby, G.C., D'Arrigo, R.D., Baatarbileg, N., Li, J.B., Curtis, A.E., 2009. A tree-ring-based drought index reconstruction for far-western Mongolia: 1565-2004. Int. J. Climatol. 29 (10), 1508–1514. https://doi.org/10.1002/joc.1798.
Du, Q., Sun, S.Z., 1990. Vegetation in the Chaidamu Basin Region and Its Utilization. Science Press, Beijing.
Eddy, J.A., 1992. The PAGES (Past Global Changes) Project: Proposed Implementation Plans for Research Activities. IGBP Global Change Report, No. 19. Sweden, Stockholm. pp. 110 pp.
Esper, J., George, S.S., Anchukaitis, K., D'Arrigo, R., Ljungqvist, F.C., Luterbacher, J., Schneider, L., Stoffel, M., Wilson, R., Büntgen, U., 2018. Large-scale, millennial-length temperature reconstructions from tree-rings. Dendrochronologia 50, 81–90. https://doi.org/10.1016/j.dendro.2018.06.001.
Fan, Z.X., Bräuning, A., Cao, K.F., 2008. Tree-Ring based drought reconstruction in the central Hengduan Mountains region (China) since A.D. 1655. Int. J. Climatol. 28 (14), 1879–1887. https://doi.org/10.1002/joc.1689.
Fang, K.Y., Gou, X.H., Chen, F.H., Liu, C.Z., Davi, N., Li, J.B., Zhao, Z.Q., Li, Y.J., 2012. Tree-ring based reconstruction of drought variability (1615-2009) in the Kongtong Mountain area, northern China. Glob. Planet. Change 80-81, 190–197. https://doi.org/10.1016/j.gloplacha.2011.10.009.
Friedrich, M., Remmele, S., Kromer, B., Hofmann, J., Spurk, M., Kaiser, K.F., Orcel, C., Küppers, M., 2004. The 12,460-year Hohenheim oak and pine tree-ring chronology from central Europe-a unique annual record for radiocarbon calibration and paleoenvironment reconstructions. Radiocarbon 46 (3), 1111–1122. https://doi.org/10.1017/s003382220003304x.
Fritts, H.C., 1976. Tree Rings and Climate. Academic Press, New York, pp. 567 pp.
Gairea, N.P., Bhujub, D.R., Koiralab, M., Shahd, S.K., Carrere, M., Timilsenaf, R., 2017. Tree-ring based spring precipitation reconstruction in western Nepal Himalaya since AD 1840. Dendrochronologia 42, 21–30. https://doi.org/10.1016/j.dendro.2016.12.004.
Gou, X.H., Chen, F.H., Jacoby, G., Cook, E., Yang, M.X., Peng, J.F., Zhang, Y., 2007. Rapid tree growth with respect to the last 400 years in response to climate warming, northeastern Tibetan Plateau. Int. J. Climatol. 27 (11), 1497–1503. https://doi.org/10.1002/joc.1480.
Gou, X.H., Deng, Y., Chen, F.H., Yang, M.X., Fang, K.Y., Gao, L.L., Yang, T., Zhang, F., 2010. Tree-ring based streamflow reconstruction for the Upper Yellow River over the past 1234 years. Chin. Sci. Bull. 55 (36), 4179–4186. https://doi.org/10.1007/s11434-010-4215-z.
Gou, X.H., Gao, L.L., Deng, Y., Chen, F.H., Yang, M.X., Still, C., 2015a. An 850-year tree-ring-based reconstruction of drought history in the western Qilian Mountains of northwestern China. Int. J. Climatol. 35 (11), 3308–3319. https://doi.org/10.1002/joc.4208.
Gou, X.H., Yang, D., Gao, L.L., Chen, F.H., Cook, E., Yang, M.X., Zhang, F., 2015b. Millennium tree-ring reconstruction of drought variability in the eastern Qilian Mountains, northwest China. Clim. Dynam. 45 (7-8), 1761–1770. https://doi.org/10.1007/s00382-014-2431-y.
Graham, N.E., Hughes, M.K., 2007. Reconstructing the Mediaeval low stands of Mono Lake, Sierra Nevada, California, USA. Holocene 17 (8), 1197–1210. https://doi.org/10.1177/0959683607085126.
Grießinger, J., Bräuning, A., Helle, G., Hochreuther, P., Schleser, G., 2016. Late Holocene relative humidity history on the southeastern Tibetan plateau inferred from a tree-ring δ18O record: recent decrease and conditions during the last 1500 years. Quat. Int. 430, 52–59. https://doi.org/10.1016/j.quaint.2016.02.011.
Grissino-Mayer, H.D., 1996. A 2129-year reconstruction of precipitation for northwestern New Mexico, USA. Dean, J.S., Meko, D.M., Swetnam, T.W. (Eds.), Tree Rings, Environment, and Humanity: Proceedings of the International Conference 191–204.
Grudd, H., Briffa, K.R., Karlén, W., Bartholin, T.S., Jones, P.D., Kromer, B., 2002. A 7400-year tree-ring chronology in northern Swedish Lapland: natural climatic variability expressed on annual to millennial timescales. Holocene 12 (6), 657–665. https://doi.org/10.1191/0959683602hl578rp.
Harris, I.C., Jones, P.D., 2017. CRU TS 4.01: Climatic Research Unit (CRU) Time-series (TS) Version 4.01 of High-resolution Gridded Data of Month-by-month Variation in Climate (Jan. 1901-Dec. 2016). Centre for Environmental Data Analysis https://doi.org/10.5285/58a8802721c94c66ae45c3baa4d814d0. 2017-12-04. [dataset].
He, M.H., Yang, B., Bräuning, A., Wang, J.L., Wang, Z.Y., 2013. Tree-ring-derived millennial precipitation record for the southern Tibetan Plateau and its possible driving mechanism. Holocene 23 (1), 36–45. https://doi.org/10.1177/0959683612450198.
He, M.H., Bräuning, A., Grießinger, J., Hochreuther, P., Wernicke, J., 2018. May-June drought reconstruction over the past 821 years on the south-central Tibetan Plateau derived from tree-ring width series. Dendrochronologia 47, 48–57. https://doi.org/10.1016/j.dendro.2017.12.006.
Hessl, A.E., Anchukaitis, K.J., Jelsema, C., Cook, B., Byambasuren, O., Leland, C., Nachin, B., Pederson, N., Tian, H., Hayles, L.A., 2018. Past and future drought in Mongolia. Sci. Adv. 4 (3), 1–7. https://doi.org/10.1126/sciadv.1701832.
Holmes, R.L., 1983. Computer-assisted quality control in tree-ring dating and measurement. Tree-Ring Bull. 43, 69–78.
Huang, J.G., Zhang, Q.B., 2007. Tree rings and climate for the last 680 years in Wulan area of northeastern Qinghai-Tibetan Plateau. Clim. Change 80 (3-4), 369–377. https://doi.org/10.1007/s10584-006-9135-1.
Hughes, M.K., Graumlich, L.J., 1996. Multimillennial dendroclimatic studies from the western United States. In: Jones, P.D., Bradley, R.S., Jouzel, J. (Eds.), Climatic Variations and Forcing Mechanisms of the Last 2000 Years. Proceedings of the NATO Advanced Research Workshop. II Ciocca, Lucca, Italy, pp. 109–124.
Kang, X.C., Zhang, Q.H., Graumlich, L.J., Sheppard, P., 2000. Reconstruction of a 1835a past climate for Dulan, Qinghai Province, using tree-ring (in Chinese). J. Glaciol. Geocryol. 22 (1), 65–72. https://doi.org/10.3969/j.issn.1000-0240.2000.01.012.
Kang, X.C., Cheng, G.D., Kang, E.S., Zhang, Q.H., 2002. Mountain pass runoff reconstruction of Heihe river during past 1000 years using tree-ring (in Chinese). Sci. China Ser. D Earth Sci. 32 (8), 675–685. https://doi.org/10.1360/zd2002-32-8-675.
Kang, X.C., Cheng, G.D., Chen, F.H., Gou, X.H., 2003. A record of drought and flood series by tree-ring data in the middle section of Qilian Mountain since 904 A.D. (in Chinese). J. Glaciol. Geocryol. 25 (5), 518–525. https://doi.org/10.3969/j.issn.1000-0240.2003.05.007.
Knight, T.A., Meko, D.M., Baisan, C.H., 2010. A bimillennial-length tree-ring reconstruction of precipitation for the Tavaputs Plateau, Northeastern Utah. Quat. Res. 73 (1), 107–117. https://doi.org/10.1016/j.yqres.2009.08.002.
Lamb, H.H., 1982. Climate, History and the Modern World. Methuen and Co. Ltd, London.
Lara, A., Wolodarsky-Franke, A., Aravena, J.C., Villalba, R., Solari, M.E., Pezoa, L., Rivera, A., Le Quesne, C., 2005. In: Huber, U.M., Bugmann, H.K.M., Reasoner, M.A. (Eds.), Climate Fluctuations Derived from Tree-Rings and Other Proxy-Records in the Chilean Andes: State of the Art and Future Prospects. Springer Netherlands, Dordrecht, pp. 145–156.
Li, T., Li, J.B., 2017. A 564-year annual minimum temperature reconstruction for the east central Tibetan Plateau from tree rings. Glob. Planet. Change 157, 165–173. https://doi.org/10.1016/j.gloplacha.2017.08.018.
Li, L., Shen, H.Y., Li, H.M., Xiao, J.S., 2015. Regional differences of climate change in Qaidam Basin and its contributing factors (in Chinese). J. Nat. Resour. 30 (4), 641–650. https://doi.org/10.11849/zrzyxb.2015.04.010.
Liu, Y., Ma, L.M., Leavitt, S.W., Cai, Q.F., Liu, W.G., 2004. A preliminary seasonal precipitation reconstruction from tree-ring stable carbon isotopes at Mt. Helan, China, since AD 1804. Glob. Planet. Change 41 (3-4), 229–239. https://doi.org/10.1016/j.gloplacha.2004.01.009.
Liu, X.H., Qin, D.H., Shao, X.M., Chen, T., Ren, J.W., 2005. Temperature variations recovered from tree-rings in the middle Qilian Mountain over the last millennium. Sci. China Ser. D: Earth Sci. 48 (4), 521–529. https://doi.org/10.1360/03yd0063.
Liu, Y., An, Z.S., Ma, H.Z., Cai, Q.F., Liu, Z.Y., Kutzbach, J.K., Shi, J.F., Song, H.M., Sun, J.Y., Yi, L., Li, Q., Yang, Y.K., Wang, L., 2006. Precipitation variation in the northeastern Tibetan Plateau recorded by the tree rings since 850 AD and its relevance to the Northern Hemisphere temperature. Sci. China Ser. D: Earth Sci. 49 (4), 408–420. https://doi.org/10.1007/s11430-006-0408-3.
Liu, X.H., Shao, X.M., Zhao, L.J., Qin, D.H., Chen, T., Ren, J.W., 2007. Dendroclimatic temperature record derived from tree-ring width and stable carbon isotope chronologies in the Middle Qilian Mountains, China. Arct. Antarct. Alp. Res. 39 (4), 651–657. https://doi.org/10.1657/1523-0430(07-506)[LIU-X]2.0.CO;2.
Liu, Y., An, Z.S., Linderholm, H.W., Chen, D.L., Song, H.M., Cai, Q.F., Sun, J.Y., Tian, H., 2009. Annual temperatures during the last 2485 years in the mid-eastern Tibetan Plateau inferred from tree rings. Sci. China Ser. D: Earth Sci. 52 (3), 348–359. https://doi.org/10.1007/s11430-009-0025-z.
Liu, J.J., Yang, B., Huang, K., Sonechkin, D.M., 2012. Annual regional precipitation variations from a 700 year tree-ring record in south Tibet, western China. Clim. Chang. Res. Lett. 53 (1), 25–41. https://doi.org/10.3354/cr01081.
Liu, Y., Lei, Y., Sun, B., Song, H.M., Li, Q., 2013. Annual precipitation variability inferred from tree-ring width chronologies in the Changling-Shoulu region, China, during AD 1853-2007. Dendrochronologia 31 (4), 290–296. https://doi.org/10.1016/j.dendro.2013.02.001.
Mann, M.E., Zhang, Z.H., Rutherford, S., Bradley, R.S., Hughes, M.K., Shindell, D., Ammann, C., Faluvegi, G., Ni, F.B., 2009. Global signatures and dynamical origins of the little ice age and medieval climate anomaly. Science 326 (5957), 1256–1260. https://doi.org/10.1126/science.1177303.
Masson-Delmotte, V., Schulz, M., Abe-Ouchi, A., Beer, J., Ganopolski, A., Rouco, J.,

Jansen, E., Lambeck, K., Luterbacher, J., Naish, T., Osborn, T., Otto-Bliesner, B., Quinn, T., Ramesh, R., Rojas, M., Shao, X.M., Timmermann, A., 2013. Information from paleoclimate archives. In: Stocker, T.F., Qin, D.H., Plattner, G.K., Tignor, M., Allen, S.K., Boschung, J., Nauels, A., Xia, Y., Bex, V., Midgley, P.M. (Eds.), Climate Change 2013: The Physical Science Basis. Contribution of Working Group I to the Fifth Assessment Report of the Intergovernmental Panel on Climate Change. Cambridge University Press, Cambridge UK and New York USA, pp. 383–464.

Michaelsen, J., 1987. Cross-validation in statistical climate forecast models. J. Appl. Meteorol. Clim. 26 (11), 1589–1600. https://doi.org/10.1175/1520-0450(1987)026<1589:CVISCF>2.0.CO;2.

Nicolussi, K., Kaufmann, M., Melvin, T.M., Van Der Plicht, J., SchieβLing, P., Thurner, A., 2009. A 9111 year long conifer tree-ring chronology for the European Alps: a base for environmental and climatic investigations. Holocene 19 (6), 909–920. https://doi.org/10.1177/0959683609336565.

Nie, C.Y., Zhang, Q.B., Lyu, L.X., 2017. Millennium-long tree-ring chronology reveals Megadroughts on the southeastern Tibetan plateau. Tree-Ring Res. 73 (1), 1–10. https://doi.org/10.3959/1536-1098-73.1.1.

Pilcher, J.R., Baillie, M.G., Schmidt, B., Becker, B., 1984. A 7,272-year tree-ring chronology for Western Europe. Nature 312, 150–152. https://doi.org/10.1038/312150a0.

Shao, X.M., Huang, L., Liu, H.B., Liang, E.Y., Fang, X.Q., Wang, L.L., 2005. Reconstruction of precipitation variation from tree rings in recent 1000 years in Delingha, Qinghai. Sci. China Ser. D: Earth Sci. 48 (7), 939–949. https://doi.org/10.1360/03yd0146.

Shao, X.M., Liang, E.Y., Huang, L., Wang, L.L., 2006. A reconstructed precipitation series over the past millennium in the Northeastern Qaidam Basin (in Chinese). Adv. Clim. Chang. Res. 2 (3), 122–126. https://doi.org/10.3969/j.issn.1673-1719.2006.03.006.

Shao, X.M., Wang, S.Z., Zhu, H.F., Xu, Y., Liang, E.Y., Yin, Z.Y., Xu, X.G., Xiao, Y.M., 2009. A 3585-year ring-width dating chronology of Qilian juniper from the northeastern Qinghai-Tibetan Plateau. IAWA J. 30 (4), 379–394. https://doi.org/10.1163/22941932-90000226.

Shao, X.M., Xu, Y., Yin, Z.Y., Liang, E.Y., Zhu, H.F., Wang, S.Z., 2010. Climatic implications of a 3585-year tree-ring width chronology from the northeastern Qinghai-Tibetan Plateau. Quat. Sci. Rev. 29 (17-18), 2111–2122. https://doi.org/10.1016/j.quascirev.2010.05.005.

Sheppard, P.R., Tarasov, P.E., Graumlich, L.J., Heussner, K.U., Wagner, M., Österle, H., Thompson, L.G., 2004. Annual precipitation since 515 BC reconstructed from living and fossil juniper growth of northeastern Qinghai Province. China. Clim. Dynam. 23 (7), 869–881. https://doi.org/10.1007/s00382-004-0473-2.

Shi, X.H., Qin, Q.S., Shao, X.M., Wang, Q.C., Liu, Y.H., 2009. Precipitation change over the past 1000 years recorded in *Sabina Tibetica* Tree Rings in Lake Qinghai Basin (in Chinese). J. Lake Sci. 21 (4), 579–586. https://doi.org/10.3321/j.issn:1003-5427.2009.04.018.

Snyder, C.W., 2010. The value of paleoclimate research in our changing climate. Clim. Change 100 (3-4), 407–418. https://doi.org/10.1007/s10584-010-9842-5.

Stokes, M.A., Smiley, T.L., 1968. An Introduction to Tree-Ring Dating. University of Chicago Press, Chicago.

Sun, J.Y., Liu, Y., 2012. Tree ring based precipitation reconstruction in the south slope of the middle Qilian Mountains, northeastern Tibetan Plateau, over the last millennium. J. Geophys. Res. 117, D08108. https://doi.org/10.1029/2011JD017290.

Sun, Y., Bekker, M.F., DeRose, R.J., Kjelgren, R., Wang, S.Y.S., 2017. Statistical treatment for the wet bias in tree-ring chronologies: a case study from the Interior West, USA. Environ. Ecol. Stat. 24 (1), 131–150. https://doi.org/10.1007/s10651-016-0363-x.

Touchan, R., Woodhouse, C.A., Meko, D.M., Allen, C., 2011. Millennial precipitation reconstruction for the Jemez Mountains, New Mexico, reveals changing drought signal. Int. J. Climatol. 31 (6), 896–906. https://doi.org/10.1002/joc.2117.

Trouet, V., Oldenborgh, G.J.V., 2013. Research tools KNMI climate explorer: a web-based research tool for high-resolution paleoclimatology. Tree-Ring Res. 69 (1), 3–13. https://doi.org/10.3959/1536-1098-69.1.3.

Wang, W.Z., Liu, X.H., Xu, G.B., Shao, X.M., Qin, D.H., Sun, W.Z., An, W.L., Zeng, X.M., 2013. Moisture variations over the past millennium characterized by Qaidam Basin tree-ring $\delta^{18}O$. Chin. Sci. Bull. 58 (32), 3956–3961. https://doi.org/10.1007/s11434-013-5913-0.

Wang, J.L., Yang, B., Chun, Q., Kang, S.Y., He, M.H., Wang, Z.Y., 2014. Tree-ring inferred annual mean temperature variations on the southeastern Tibetan Plateau during the last millennium and their relationships with the Atlantic Multidecadal Oscillation. Clim. Dynam. 43 (3-4), 627–640. https://doi.org/10.1007/s00382-013-1802-0.

Wang, J.L., Yang, B., Ljungqvist, F.C., 2015. A millennial summer temperature reconstruction for the eastern Tibetan plateau from tree-ring width. J. Clim. 28 (13), 5289–5304. https://doi.org/10.1175/JCLI-D-14-00738.1.

Warren, W.G., 1980. On removing the growth trend from dendrochronological data. Tree-Ring Bull. 40, 35–43.

Wigley, T.M., Briffa, K.R., Jones, P.D., 1984. On the average value of correlated time series, with applications in dendroclimatology and hydrometeorology. J. Clim. Appl. Meteorol. 23 (2), 201–213. https://doi.org/10.1175/1520-0450(1984)023<0201:OTAVOC>2.0.CO;2.

Xu, Y., Shao, X.M., 2007. Standardization of Qilian Juniper ring-width series in the eastern margin of the Qaidam Basin. J. Geogr. Sci. 17 (2), 175–186. https://doi.org/10.1007/s11442-007-0175-x.

Xu, C., Zheng, H., Nakatsuka, T., Sano, M., Li, Z., Ge, J., 2016. Inter- and intra-annual tree-ring cellulose oxygen isotope variability in response to precipitation in Southeast China. Trees-Struct. Funct. 30 (3), 785–794. https://doi.org/10.1007/s00468-015-1320-2.

Yang, B., Qin, C., Wang, J.L., He, M.H., Melvin, T.M., Osborn, T.J., Briffa, K.R., 2014. A 3500-year tree-ring record of annual precipitation on the northeastern Tibetan Plateau. Proc. Natl. Acad. Sci. U. S. A. 111 (8), 2903–2908. https://doi.org/10.1073/pnas.1319238111.

Yin, Z.Y., Shao, X.M., Qin, N.S., Liang, E.Y., 2008. Reconstruction of a 1436-year soil moisture and vegetation water use history based on tree-ring widths from Qilian junipers in northeastern Qaidam Basin, northwestern China. Int. J. Climatol. 28 (1), 37–53. https://doi.org/10.1002/joc.1515.

Yin, Z.Y., Zhu, H.F., Huang, L., Shao, X.M., 2016. Reconstruction of biological drought conditions during the past 2847 years in an alpine environment of the northeastern Tibetan Plateau, China, and possible linkages to solar forcing. Glob. Planet. Change 143, 214–227. https://doi.org/10.1016/j.gloplacha.2016.04.010.

Yu, J., Liu, Q.J., Meng, S.W., Zhou, G., Shah, S., Xu, Z.Z., 2018. Summer temperature variability inferred from tree-ring records in the central Hengduan Mountains, southeastern Tibetan Plateau. Dendrochronologia 51, 92–100. https://doi.org/10.1016/j.dendro.2018.08.004.

Zhang, Q.B., Qiu, H.Y., 2007. A millennium-long tree-ring chronology of *Sabina Przewalskii* on northeastern Qinghai-Tibetan Plateau. Dendrochronologia 24 (2-3), 91–95. https://doi.org/10.1016/j.dendro.2006.10.009.

Zhang, Q.B., Cheng, G.D., Yao, T.D., Kang, X.C., Huang, J.G., 2003. A 2326-year tree-ring record of climate variability on the northeastern Qinghai-Tibetan Plateau. Geophys. Res. Lett. 30 (14), 1739–1741. https://doi.org/10.1029/2003GL017425.

Zhang, P.Z., Cheng, H., Edwards, R.L., Chen, F.H., Wang, Y.J., Yang, X.L., Liu, J., Tan, M., Wang, X.F., Liu, J.H., 2008. A test of climate, sun, and culture relationships from an 1810-year Chinese cave record. Science 322 (5903), 940–942. https://doi.org/10.1126/science.1163965.

Zhang, T.W., Wang, L.L., Yuan, Y.J., Wei, W.S., Yu, S.L., Zhang, R.B., Chen, F., Shang, H.M., Fan, Z.A., 2011a. A 645-year precipitation reconstruction in Baluntai region on southern slope of mid-Tianshan Mountains based on tree-ring width (in Chinese). Sci. Geogr. Sin. 31 (2), 251–256. https://doi.org/10.13249/j.cnki.sgs.2011.02.005.

Zhang, Y., Tian, Q.H., Gou, X.H., Chen, F.H., Leavitt, S.W., Wang, Y.S., 2011b. Annual precipitation reconstruction since AD 775 based on tree rings from the Qilian Mountains, northwestern China. Int. J. Climatol. 31 (3), 371–381. https://doi.org/10.1002/joc.2085.

Zhang, Y., Shao, X.M., Yin, Z.Y., Wang, Y., 2014. Millennial minimum temperature variations in the Qilian Mountains, China: evidence from tree rings. Clim. Past 10 (5), 1763–1778. https://doi.org/10.5194/cp-10-1763-2014.

Zhao, X.Y., Zheng, Z.W., Shang, Z.Y., Wang, J., Cheng, R.Q., Qian, J.L., 2014. Climatic information recorded in stable carbon isotopes in tree rings of Cryptomeria fortunei, Tianmu Mountain, China. Dendrochronologia 32 (3), 256–265. https://doi.org/10.1016/j.dendro.2014.06.002.

Zheng, D., 1996. The system of physico-geographical regions of the Qinghai-Xizang (Tibet) Plateau. Sci. China Ser. D: Earth Sci. 39 (4), 410–417. https://doi.org/10.1360/yd1996-39-4-410.

Zhu, H.F., Zheng, Y.H., Shao, X.M., Liu, X.H., Xu, Y., Liang, E.Y., 2008. Millennial temperature reconstruction based on tree-ring widths of Qilian juniper from Wulan, Qinghai Province, China. Chin. Sci. Bull. 53 (24), 3914–3920. https://doi.org/10.1007/s11434-008-0400-8.